JOURNAL OF CATALYSIS 65, 461–469 (1980)

Adsorption of Oxygen on Pt(111) and Its Reactivity to Hydrogen and Carbon Monoxide

DAVID R. MONROE[1] AND ROBERT P. MERRILL

School of Chemical Engineering,[2] Cornell University, Ithaca, New York 14850

Received October 4, 1978; revised February 25, 1980

Oxygen was found to adsorb on Pt(111) with an initial sticking coefficient of 0.048 ± 0.006 and linear adsorption kinetics. The surface saturated at an oxygen to platinum ratio of 1:4. The reactivity of adsorbed oxygen to hydrogen and CO was determined from steady-state oxygen coverages for H_2–O_2 and CO–O_2 mixtures. From the reactivity data which show reaction probabilities of 1.0 for CO and $\frac{1}{2}$ for H_2 over a wide range of oxygen coverages, it is concluded that both H_2 and CO are reactive in mobile states which may be the precursors to adsorption.

I. INTRODUCTION

Oxygen adsorption on platinum has been investigated many times; however, no clear comprehensive understanding is yet available. This work has been undertaken to try to gain a greater understanding of the platinum–oxygen system and hopefully to reconcile some of the widely divergent results previously reported. The (111) face of platinum selected for this work is the most stable of the platinum surfaces and X-ray analysis of platinum ribbons has frequently shown that the majority of the surface is (111).

Spicer *et al.* (*1*), working on polycrystalline platinum, found oxygen to be atomically adsorbed with a binding energy of about 40 kcal/mole. The oxygen had an initial sticking coefficient of 0.05 and the surface saturated at 1 atom of oxygen per 4 surface atoms of platinum. Tucker (*2*) obtained a (2 × 2) low-energy electron diffraction pattern on Pt(111) following exposure to oxygen while Lang *et al.* (*3*) and Lampton (*4*) found no change in the diffraction pattern. Weinberg *et al.* (*5*) found a sticking coefficient of 7×10^{-7} for oxygen on the (111) face. However, Stoll and Merrill (*6*) found the sticking coefficient to be greater than 0.01 on this face and found that oxygen adsorption resulted in a (2 × 2) LEED pattern. They also found that the oxygen was rapidly removed by reaction with background gases and that the rate of removal was inconsistent with the Eley–Rideal mechanism (reaction between an adsorbed species and a gaseous species). Bonzel and Ku (*7*), also working on Pt(111), found an initial sticking coefficient of 0.1 that was temperature independent between 214 and 400°C. The oxygen adsorption rate varied inversely with the exponential of the surface coverage and the surface saturated at 1 atom of oxygen per 2 surface platinum atoms. From the rate of removal of the adsorbed oxygen by CO they concluded that the reaction was between adsorbed oxygen and gas-phase CO (Eley–Rideal mechanism). Collins and Spicer (*8*) found that Pt(111) had a saturation coverage of 1 oxygen atom per 25 surface platinum atoms. Gland (*9*) has found an initial sticking coefficient of 0.05 at −73°C for oxygen on Pt(111) and an initial saturation of 1 oxygen to 4 surface platinum atoms. This saturation could be increased by thermal cycling. Ducros and Merrill (*10*) found an initial sticking coefficient of 0.4 for oxygen on the Pt(110) face.

[1] Current address: General Motors Research Laboratories, Warren, Mich. 48090.

[2] Work performed at the University of California, Berkeley.

0021-9517/80/100461-09$02.00/0

Hydrogen adsorption on polycrystalline platinum and Pt(111) has been studied by Norton (*11*) and Lampton (*4*), respectively. In both studies the bare surface sticking coefficient was found to decrease with increasing surface temperature. Norton found values of 0.43 at −196°C falling to 0.09 at 0°C while Lampton found 0.1 at 45°C falling to 0.015 at 150°C.

Carbon monoxide adsorption onto Pt(111) was studied by Comrie (*12*) and found to have an initial sticking coefficient of 0.52. The sticking coefficient remains large over a wide range of CO surface concentrations. This suggests that the CO is first adsorbed into a mobile precursor state (*13*). Since the CO is highly mobile it can diffuse over a large surface area and the sticking coefficient does not decrease until the time it takes for the CO to be chemically adsorbed becomes significant relative to the time for the precursor to desorb.

II. EXPERIMENTAL PROCEDURES

The vacuum chamber used in these experiments was a 200-liter stainless-steel chamber equipped with a 400 l/s ion pump and a titanium sublimation pump. The system had a quadrupole mass spectrometer, a coaxial cylindrical-mirror Auger electron spectrometer, and a Faraday cup low-energy electron diffraction unit. Background pressures of 4×10^{-11} Torr were obtained; however, backgrounds of 2×10^{-10} Torr were more typical during the course of the experimental work.

Two variable leak valves were connected to the vacuum system to allow easy control of two gas pressures. The gases used in these experiments were all research grade and greater than 99.9% purity.

The Pt(111) crystal used was cut from a platinum rod of 99.9% purity purchased from Materials Research Corporation. The crystal was oriented using Laue back-diffraction and cut on a spark cutter. The crystal was then polished using four grades of abrasive paper followed by 1 μm alumina slurry. Subsequent examination in the vacuum chamber has shown the crystal to be within $\frac{1}{2}^\circ$ of the (111) plane as evidenced by the lack of spot splitting in the LEED pattern (*14*).

The crystal was cleaned in an ultrasonic bath of methylethyl ketone, then boiled in a 50% solution of hydrochloric acid, and washed in distilled water. It was then cleaned in acetone and in ethanol before being placed in the vacuum chamber. The crystal was cleaned *in situ* by heating to 1000°C for 24 hr in 1×10^{-7} Torr of oxygen. The oxygen was removed by flashing the crystal to 1300°C. The AES showed no detectable carbon, calcium, phosphorus, sulfur, or oxygen. All the observed features could be indexed to known Auger transitions for Pt.

III. RESULTS

Before measuring the oxygen sticking coefficient the surface was cleaned by flashing to 1300°C. While the crystal was cooling AES was taken to verify that the surface was clean and to calibrate the AES by measuring the height of the Pt_{237} peak. When the crystal had cooled to 100°C (about 4 min after the flash) oxygen was leaked into the system and height of the O_{510} peak monitored by continuous AES scans. The resulting adsorptions for pressures of 9×10^{-9} and 6.2×10^{-8} Torr are shown in Fig. 1, where the calibration of Bonzel and Ku[3] has been used to convert the peak height ratios to surface coverage. The maximum coverage obtained was 3.6×10^{14} atoms oxygen/cm^2. A monolayer coverage ($\theta = 1$) was defined as 3.76×10^{14} atoms/cm^2 since this corresponds to a platinum to oxygen surface ratio of 4:1 and is compatible with the (2 × 2) LEED patterns observed. The same procedure was repeated for a crystal temperature of 385°C and 6.2×10^{-8} Torr of oxygen and is also plotted in Fig. 1.

At 100°C the height of the oxygen peak

[3] $O_{510}/Pt_{235} = 0.65 = 1.505 \times 10^{15}$ oxygen atoms/cm^2 (*7*).

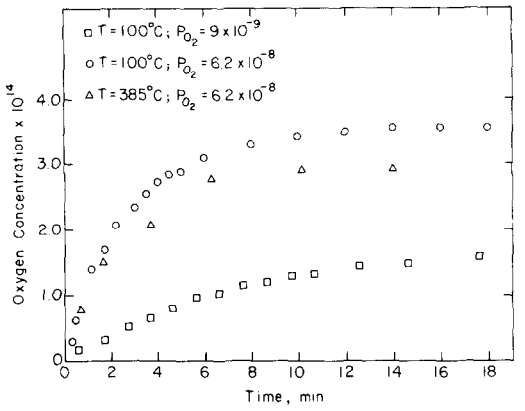

FIG. 1. Adsorbed oxygen concentration vs time for different crystal temperature and oxygen pressures.

reached a steady-state height after about 10 min. This peak remained unchanged if the beam was moved to a different spot on the crystal and the O_{510}/Pt_{235} ratio was independent of beam current. This indicates that at 100°C the surface oxygen concentration is unaffected by the AES beam.

At 385°C, however, moving the crystal did cause the oxygen peak to rise and then decline over a period of 3 min. To quantify the effect of the Auger electron beam upon the surface oxygen concentration the steady-state oxygen concentration was measured as a function of beam current. Assuming first-order processes for oxygen adsorption and removal of oxygen by the Auger beam, one may write for the steady-state condition

$$ki\theta(i) = 1 - \theta(i), \qquad (1)$$

k = proportionality constant for 5×10^{-8} Torr O_2, 385°C,
i = Auger beam current, and
$\theta(i)$ = measured surface coverage,

which rearranges to

$$ki = -1 + 1/\theta(i). \qquad (2)$$

In Fig. 2 the Auger beam current, i, is plotted vs $-1 + 1/\theta(i)$ for a surface temperature of 385°C. The resulting plot is linear as expected from (2).

Initial attempts to obtain oxygen adsorption data as a function of time at 100°C resulted in a maximum surface oxygen concentration after 20 min and then a slow decline. After 1 hr the surface oxygen concentration was only about 10% of its maximum value. This phenomena was noted both with the Auger beam on continuously and with the beam on for 30 sec every 20 min, indicating it was not induced by the electron beam. A similar phenomena has been noted on the (110) surface (*17*). This decline was accompanied by an increase in the Pt_{390} AES peak. This peak eventually split into two peaks, the Pt_{390} peak and a peak at about 380 V. The mass spectrometer indicated the presence of a small quantity of NO. Frequent flashing and constant cooling of the titanium sublimation pump during the adsorption measurements produced data like those shown in Fig. 1. During these adsorptions there is no decline in the measured oxygen concentration or growth of either the 390- or 380-V peak and there was no evidence of NO in the mass spectrum. Nitrogen has a strong Auger transition at 381 V (*15*). If indeed the presence of nitrogen is responsible for this decline in the O_{510} Auger transition, the mechanism is certainly obscure. It is emphasized, however, that adsorptions like those shown in Fig. 1 cannot be obtained without continuous and careful gettering in the vacuum system.

The reactivity of adsorbed oxygen was

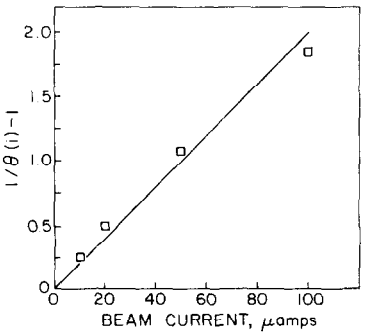

FIG. 2. Steady-state surface oxygen coverage vs AES beam current at 385°C and 6.2×10^{-8} Torr of oxygen.

measured by changes in the steady-state surface oxygen concentration as a function of reducing gas concentration. The crystal was flashed to 1300°C and then adjusted to 385°C. Either hydrogen or CO was leaked into the vacuum system through one leak valve and the system pressure then raised to 1.2×10^{-7} Torr by leaking oxygen in through a second leak valve. The AES beam was initially off to minimize CO decomposition on the surface. After 10 min, it was turned on with an emission of 10 μA and the Pt_{235} peak measured. Fourteen minutes after starting the oxygen (100-Langmuir exposure) the O_{510} peak was measured and the oxygen, hydrogen, and CO partial pressures measured with the mass spectrometer. This provided the steady-state surface oxygen concentrations as a function of the oxygen, hydrogen, and CO partial pressures shown in Fig. 3. At low fluxes of hydrogen and CO the oxygen coverage is less for the CO, indicating the CO is more reactive than the H_2. However, at higher fluxes of reducing gas, the coverage is slightly less for the hydrogen than for the CO.

IV. DISCUSSION

A. Oxygen Adsorption

The adsorption data shown in Fig. 1 indicate an adsorption in which the rate of adsorption is proportional to the amount of oxygen-free surface, suggesting the adsorption rate equation:

$$\frac{d\theta}{dt} = \frac{2F_{O_2} \cdot S}{N}(1 - \theta) - \alpha \cdot \theta, \qquad (3)$$

θ = fractional surface coverage,
F_{O_2} = molecular oxygen flux rate,
S = sticking coefficient,
N = number of oxygen adsorption sites/cm^2,
α = parameter to account for oxygen removal.

The term $\alpha \cdot \theta$ was included since the steady-state coverage is affected by both the AES beam and the hydrogen and CO present in the background gas. It will be shown later that above about 2×10^{14} oxygen atoms/cm^2 the reaction probability becomes independent of surface oxygen concentration; however, this introduced a negligible error. For example, the removal at 100°C and 6.2×10^{-8} Torr (see Fig. 1) was not significant because the background partial pressure of reducing gases was very low compared to the oxygen partial pressure. At 385°C, the removal was predominantly initiated by the electron beam, and is therefore proportional to θ as demonstrated by the data of Fig. 2. Thus a number of adsorptions that could be expected to follow Eq. (1) could be identified. The factor α was never explicitly calculated but was included with other terms in the solution of

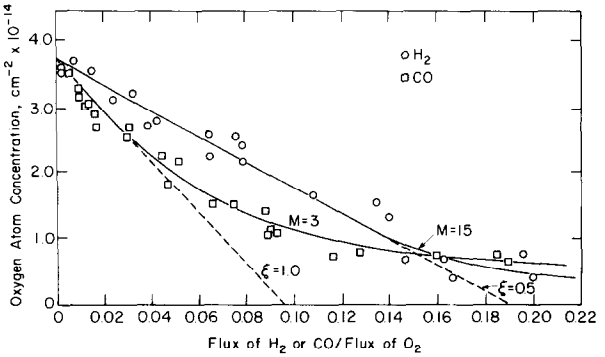

FIG. 3. Adsorbed oxygen concentration after 100-Langmuir exposure to mixture of either H_2 and O_2 or CO and O_2.

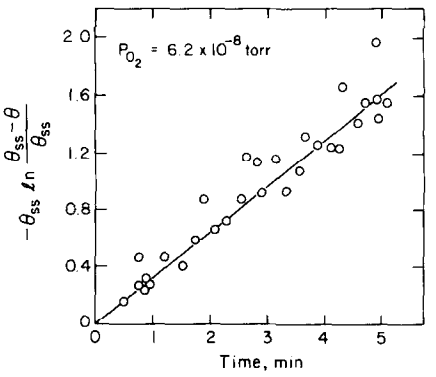

FIG. 4. Surface coverage of oxygen as a linearized function of time.

the rate equation in terms of the steady-state oxygen coverage, which is given by

$$\theta_{ss} = 2F_{O_2} \cdot S/(2F_{O_2} \cdot S + \alpha \cdot N), \quad (4)$$

and is easily determined from adsorption data like those in Fig. 1. Equation (3) can be solved to give

$$\frac{2F_{O_2} \cdot S}{N} \cdot t = -\theta_{ss} \ln \frac{\theta_{ss} - \theta}{\theta_{ss}}. \quad (5)$$

The adsorption data taken at 6.2×10^{-8} Torr of oxygen at 100 and 385°C have been linearized according to Eq. (5) and are plotted in Fig. 4, using the maximum coverage obtained in each adsorption as θ_{ss}. The maximum surface concentration of oxygen encountered was 3.68×10^{14} atoms/cm^2. A value of 3.76×10^{14} sites/cm^2 was chosen for N. This corresponds to 1 oxygen site per 4 surface platinum atoms and is assumed to be a "monolayer" in the following discussion. A uniform distribution of oxygen atoms over the surface at this concentration would give a (2 × 2) LEED pattern, and a (2 × 2) LEED pattern was observed following these oxygen adsorptions.

The sticking coefficient, S, was 0.048 ± 0.006 as computed from the slope of the data in Fig. 4. This value is predicted, of course, upon the assumption of linear adsorption kinetics. The sticking coefficient, however, could also be computed from the initial slope of the low-pressure data like those in Fig. 1. This resulted in a value of 0.045 ± 0.01 for the bare surface sticking coefficient, which agrees well with that calculated from Fig. 4.

Figure 5 shows adsorption data taken at 100°C and 6.2×10^{-8} Torr along with calculated adsorptions from three different types of adsorption kinetics: linear kinetics, second-order kinetics, and exponential kinetics. The second-order kinetics were investigated because it is the commonly expected form for the random dissociative chemisorption of a diatomic molecule. The exponential form would be applicable if there were an activation energy for adsorption in which the barrier is a function of surface coverage. This form was used by

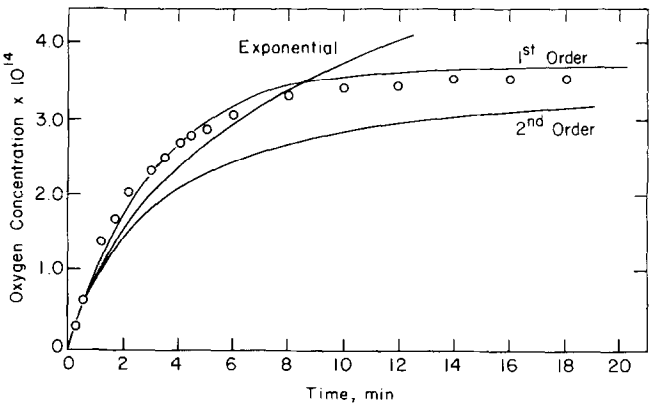

FIG. 5. Oxygen adsorption data fitted to first-order, second-order, and exponential adsorption kinetics.

Bonzel and Ku (*7*) to fit their oxygen adsorption on Pt(111) data. The initial slopes of all three forms were set to give an initial sticking coefficient of 0.045. This completely established the first- and second-order forms. A second parameter, the rate of change of the activation barrier with the surface coverage, was required by the exponential form and was adjusted to give the best fit of the data. Figure 5 clearly shows the second-order and exponential kinetics to be inappropriate for these data. The small differences between the data and first-order calculations at long times can be attributed quantitatively to oxygen removal by reactions with hydrogen and CO present in the background gas.

Oxygen has been shown by Spicer *et al.* (*1*) to be atomically adsorbed, which would suggest second-order adsorption kinetics. That first-order kinetics apply indicates that oxygen adsorption probably occurs either through a precursor state or through an undissociated transition state. Weinberg *et al.* (*5*) calculated a maximum sticking coefficient of 0.002 for oxygen on Pt(111), assuming that the oxygen passed directly from the gas phase into an immobile surface state. The sticking coefficient measured here is 25 times larger than the maximum of Weinberg *et al.*, indicating that the oxygen cannot pass directly from the gas phase into an immobile surface state and that it must pass either through a precursor state or through a mobile transition state. This supports the evidence from the concentration dependence of the sticking coefficient that the slow step in the adsorption event occurs before dissociation.

B. Reactions with Reducing Gases

The steady-state oxygen concentration for mixtures of either oxygen and CO or oxygen and hydrogen at 385°C is shown in Fig. 3. The surface coverages shown are the measured values corrected for the effect of the AES beam via Eq. (2) and the data in Fig. 2. The surface temperature is well above the desorption temperature of hydrogen and CO so the only adsorbed species on the surface would be oxygen and, as shown previously,

$$\text{rate of oxygen adsorption} = 2F_{O_2}S(1 - \theta).$$

At steady state the rate of oxygen adsorption is equal to the rate of reaction:

$$\text{rate of reaction} = F_{H_2}\phi_{H_2} + F_{CO}\phi_{CO},$$

where the ϕ's are reaction probabilities. Then for one reducing gas:

$$\phi_R = 2F_{O_2}S(1 - \theta)/F_R.$$

The unknown function ϕ_R can be computed from the measured steady-state oxygen coverages. In the oxygen–CO system the surface oxygen concentration initially falls as a linear function of the oxygen to CO flux ratio with a slope implying a unity reaction probability. At approximately one-half of a monolayer ($2 \times 10^{14}/cm^2$) the reaction probability, ϕ_R, becomes a function of the surface oxygen coverage, θ. That the reaction probability should be independent of surface coverage down to half a monolayer or about 53 Å^2/oxygen atom indicates a very large reactive cross section. This large cross section suggests that the CO is adsorbed into a mobile surface state that will allow it to diffuse to the oxygen. While it cannot be ruled out, it is considered unlikely that oxygen diffusion occurs rapidly enough to explain these results. It has a higher heat of desorption (about 40 kcal vs about 30 for CO) and a sharp and intense LEED pattern, both of which suggest low surface mobility.

The large cross section suggests a model in which the reaction probability, ϕ_{CO}, is given by the product of the probability of adsorption into a reactive state times the probability that it will find an oxygen atom within the reactive cross section:

$$\phi_{CO} = \zeta_{CO}[1 - (1 - \theta)^M]. \qquad (6)$$

Here M is the number of oxygen adsorption sites within the reaction cross section. $(1 - \theta)^M$ represents the probability that all of

these sites are vacant; hence $1 - (1 - \theta)^M$ is the probability that there is at least one oxygen atom within the reactive cross section. ζ_{CO} is the probability that the CO is adsorbed from the gas phase into a reactive precursor state and is given by the slope of the reaction probability at $\theta = 1$. For the CO–oxygen system, $\zeta = 1.0$ and $M = 3$, which corresponds to a reactive cross section of 80 Å^2. With hydrogen and oxygen, $\zeta = 0.5$, $M = 15$, and the reactive cross section is 400 Å^2. The reactive cross section, as it is used here, is an average area through which the reducing gas in the reactive precursor state can diffuse before being reemitted to the gas phase.

Lampton (*4*) reports a value of 0.015 for the sticking coefficient of hydrogen on Pt(111) above 150°C, which is over two orders of magnitude lower than ζ_{H_2}. Thus, the reactive surface state for hydrogen differs from its final adsorbate state. The value for ζ_{CO} is also greater than what has been reported for the sticking coefficient of CO on Pt(111) (about 0.5) (*10, 11*).

The sticking coefficient of hydrogen on platinum has been shown to decrease with increasing temperature. This can easily be explained by assuming that hydrogen adsorbs on platinum through a precursor state. The energy barrier for adsorption from the precursor state is less than that for desorption (Fig. 6). For a hydrogen molecule in such a precursor state the rate of desorption using transition-state theory is given by (*16*)

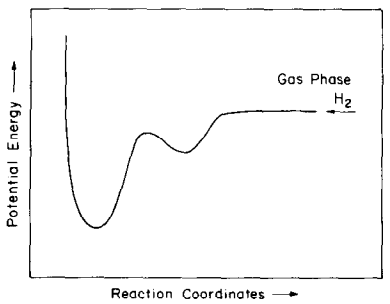

FIG. 6. Reaction coordinate vs potential for hydrogen adsorbing through a precursor state.

$$r_d = \frac{kT}{h} Q_d^*/Q_p \exp\{-E_d/kT\}, \quad (7)$$

Q_d^* = desorption transition-state partition function,
Q_p = precursor-state partition function,
E_d = activation energy for desorption;

and for adsorption from the precursor:

$$r_a = \frac{kT}{h} Q_a^*/Q_p \exp\{-E_a/kT\}, \quad (8)$$

Q_a^* = adsorption transition-state partition function,
r_a = activation energy for adsorption.

These absolute rates cannot be calculated since neither E_d nor E_a is known. However, if the incident hydrogen flux (F_{H_2}) is trapped into the precursor state with a trapping probability, γ, a steady state with a precursor concentration of (P) would be isolated. Hence:

$$\frac{d(P)}{dt} = r_a(P) + r_d(P) - \gamma F_{H_2} = 0,$$

$$r_a/r_d = \gamma F_{H_2}/r_d(P) - 1. \quad (9)$$

The rate of desorption is equal to the trapping probability (into the precursor state) minus the sticking probability, S, times the incident flux:

$$r_d(P) = (\gamma - S)F_{H_2}. \quad (10)$$

Substituting Eq. (10) into Eq. (9)

$$r_a/r_d = \frac{1}{1 - S/\gamma} - 1, \quad (11)$$

$$r_a/r_d = S/\gamma + S^2/\gamma^2 + S^3/\gamma^3 \cdots . \quad (12)$$

For small S, $r_a/r_d \simeq S/\gamma$, but from Eqs. (7) and (8)

$$r_a/r_d = Q_a^*/Q_d \exp -(E_d + E_a)/kT. \quad (13)$$

A semilogarithmic plot of Lampton's sticking coefficient versus $1/T$ (Fig. 7) shows that $(E_d - E_a)$ is 5.6 kcal and at 100°C $S = 0.03$. Therefore:

$$Q_a^*/Q_d^* = 0.03/\gamma e^{-5600/RT}. \quad (14)$$

The adsorbed state is probably very local-

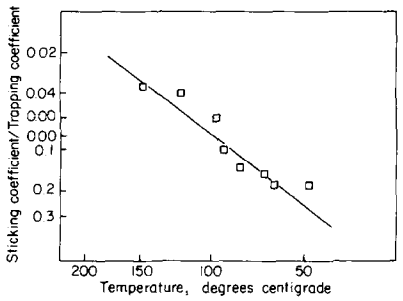

FIG. 7. Arrhenius plot of hydrogen sticking coefficient (*4*), divided by trapping probability (assumed 0.5).

ized relative to the precursor state so that the smallest possible partition function for this species would contain only vibrational motion and hence have a value of unity. The largest possible partition function for the transition state for the desorption step would have two degrees of translational freedom and two degrees of rotational freedom:

$$Q_d^* = q_t^2 q_r^2, \tag{15}$$

$$q_r^2 = d_{H_2} m_{H_2} 4\pi kT/h^2, \tag{16}$$

$$d_{H_2} = 0.746 \text{ Å}. \tag{17}$$

At 100°C q_r^2 is 8.636. The translational partition function q_t^2 is given by:

$$q_t^2 = 2m_{H_2}\pi kT/h^2 A, \tag{18}$$

where A is the area of intersection between the surface and the desorbing gas. At 100°C

$$q_t^2 = 2.46 \times 10^{16} A. \tag{19}$$

The trapping coefficient γ must be less than 1 and, since Lampton measured a sticking coefficient of 0.1 at 20°C, must be greater than 0.1. If γ is only a weak function of surface temperature, A, the area of interaction, can be calculated to be between 290 and 2900 Å^2. If the transition state for the adsorption step were not completely mobile and/or the transition state for the desorption step hindered with respect to either rotation or translation, then the area would be proportionally larger.

This area of interaction as measured by the hydrogen adsorption data is consistent with the results of the hydrogen reactivity. The reactivity data showed that hydrogen was diffusing over an area of 400 Å^2 with a unity reaction probability and a 0.5 probability of entering this mobile state. If it is assumed that the mobile state for adsorption is the same as for reaction, then the trapping coefficient, γ, can be set equal to 0.5, the value for high oxygen coverage, and the apparent area of the adsorbate is 1450 Å. This seems to be adequate agreement considering the approximate nature of the transition-state model.

V. CONCLUSIONS

Oxygen is adsorbed on platinum(111) with an initial sticking coefficient of 0.05 and at a rate that is proportional to the amount of oxygen-free surface. The surface saturates at a coverage of 1 oxygen atom per 4 platinum atoms. At 385°C this adsorbed oxygen is very reactive to both hydrogen and CO, the oxygen-saturated surface having a reaction probability of 1.0 for CO and 0.5 for hydrogen. These reaction probabilities remain constant until the surface oxygen concentration has fallen to one-half its saturation level for reduction by CO and to one-fifth its saturation level for reduction by hydrogen. These high reactivities at low oxygen coverages cannot be explained by a reaction upon impact between adsorbed oxygen and gas-phase hydrogen (Eley–Rideal mechanism) or CO and indicate that the reaction takes place between two surface species at least one of which is mobile. The reaction probabilities for the reducing gases are also well above their sticking coefficients. Since both hydrogen and CO adsorptions on platinum are indicative of adsorption through a mobile precursor state, the precursor state is probably the reactive state for interaction with adsorbed oxygen.

There are at least two possible sources of error in the determination of the oxygen sticking coefficient: oxygen removal by reaction before detection, and surface de-

fects. The reaction probability of adsorbed oxygen to hydrogen and CO, two common vacuum chamber background gases, is more than 10 times greater than the oxygen sticking coefficient over a wide range of surface oxygen concentrations, and can, under some conditions, remove adsorbed oxygen at a rate sufficient to make oxygen adsorption appear substantially slower than it actually is. Oxygen is also more easily adsorbed on high-index stepped platinum(111) faces than on the unstepped surfaces (*3*). The sticking coefficient found by Ducros and Merrill (*10*) on the atomically rough Pt(110) was 8 times that found here for the atomically smooth Pt(111). Since the full range of oxygen adsorption could be well represented by the sticking coefficient and linear kinetics, it is believed that defects were only a small fraction of the total surface and did not play a significant role in the work. These two factors, the presence of atomic defects and removal of adsorbed oxygen by CO and H_2 in the background gas, can account for much of the disparity in previously published results.

ACKNOWLEDGMENTS

This work was sponsored by AFOSR Grant 76-2926 and by NASA Contract NSG-1347.

REFERENCES

1. Spicer, W. E., Collins, D. M., and Lee, J. B., paper presented at Amer. Chem. Soc. Meeting, Mexico City, December 1975.
2. Tucker, C. W., *J. Appl. Phys.* **35,** 1897 (1964).
3. Lang, B., Joyner, R. W., and Somorjai, G. A., *Surface Sci.* **30,** 454 (1974).
4. Lampton, V., M.S. Thesis, University of California, 1971.
5. Weinberg, W. H., Lambert, R. M., Comrie, C. M., and Linnett, J. W., *Surface Sci.* **30,** 299 (1972).
6. Stoll, A. G., Ph.D. thesis, University of California, 1973.
7. Bonzel, H. P., and Ku, R., *Surface Sci.* **40,** 85 (1976); **33,** 91 (1973).
8. Collins, D. M., and Spicer, W. E., *Surface Sci.* 69–85 (1972).
9. Gland, J. L., private communication, to be submitted to *Surface Sci.*
10. Ducros, R., and Merrill, R. P., *Surface Sci.* **55,** 277 (1976).
11. Norton, P. R., *Surface Sci.* **44,** 129 (1974).
12. Comrie, C. M., Ph.D. thesis, University of Cambridge, 1974.
13. Weinberg, W. H., Comrie, C. M., and Lambert, R. M., *J. Catal.*
14. Henzler, M., *Surface Sci.* **19,** 159 (1970).
15. Palmberg, Riech, Weber, and McDonald, "Handbook of Auger Electron Spectroscopy." Physical Electronics Industries, Edina, Minn., 1972.
16. Laidler, K. J., "Chemical Kinetics," Chap. 3. McGraw–Hill, New York, 1965.
17. Schmidt, L., private communication.